Title

Arylthiazole antibiotics targeting intracellular methicillin-resistant Staphylococcus aureus (MRSA) that interfere with bacterial cell wall synthesis

Authors

Eid, Islam
Elsebaei, Mohamed M
Mohammad, Haroon
et al.

Publication Date

2017-10-01

DOI

10.1016/j.ejmech.2017.08.039

Peer reviewed

HHS Public Access

Author manuscript

Eur J Med Chem. Author manuscript; available in PMC 2018 April 23.

Published in final edited form as:

Eur J Med Chem. 2017 October 20; 139: 665–673. doi:10.1016/j.ejmech.2017.08.039.

Arylthiazole Antibiotics Targeting Intracellular Methicillin-resistant *Staphylococcus aureus* (MRSA) that Interfere with Bacterial Cell Wall Synthesis

Islam Eid[1], **Mohamed M. Elsebaei**[1], **Haroon Mohammad**[2], **Mohamed Hagras**[1], **Christine E. Peters**[3], **Youssef A. Hegazy**[2], **Bruce Cooper**[4], **Joe Pogliano**[3], **Kit Pogliano**[3], **Hamada S. Abulkhair**[1], **Mohamed N. Seleem**[2,5], and **Abdelrahman S. Mayhoub**[1,6,*]

[1]Department of Organic Chemistry, College of Pharmacy, Al-Azhar University, Cairo 11884, USA

[2]Department of Comparative Pathobiology, Purdue University, College of Veterinary Medicine, West Lafayette, IN 47907, USA

[3]Division of Biological Sciences, University of California, San Diego, La Jolla, CA, USA

[4]Bindley Bioscience Center, Purdue University, West Lafayette, IN, USA

[5]Purdue Institute for Inflammation, Immunology, and Infectious Diseases, West Lafayette, IN 47907, USA

[6]Biomedical Sciences, University of Science and Technology, Zewail City of Science and Technology, Giza, Egypt

Abstract

The promising antibacterial potency of arylthiazole antibiotics is offset by their limited activity against intracellular bacteria (namely methicillin-resistant *Staphylococcus aureus* (MRSA)), similar to many clinically-approved antibiotics. The failure to target these hidden pathogens is due to the compounds' lack of proper characteristics to accumulate intracellularly. Fine tuning of the size and polar-surface-area of the linking heteroaromatic ring provided a new series of 5-thiazolylarylthiazoles with balanced properties that allow them to sufficiently cross and accumulate inside macrophages infected with MRSA. The most promising compound **4i** exhibited rapid bactericidal activity, good metabolic stability and produced over 80% reduction of intracellular MRSA in infected macrophages.

Keywords

antibiotic drug resistance; *Caenorhabditis elegans*; Methicillin-resistant *Staphylococcus aureus*; MRSA; intracellular infection; pharmacokinetics

[*]**Corresponding Authors.** ASM; amayhoub@azhar.edu.eg; MNS; mseleem@purdue.edu.

1. INTRODUCTION

The consistent upward trend in antibiotic resistance threatens to undermine the entire structure of modern medicine which relies heavily on widespread use of antibiotics to curb bacterial infections, particularly in healthcare settings. Without escalating the discovery and approval of new antibiotics and introducing new scaffolds with the ability to combat the rapid rise in bacterial resistance to traditional classes of antibiotics, we risk moving back towards the pre-antibiotic era. One particularly problematic pathogen is methicillin-resistant *Staphylococcus aureus* (MRSA)[1] which is classified as a *serious threat* by the U.S. Centers for Disease Control and Prevention.[2] MRSA has several mechanisms to evade the host immune system and the effect of antibiotics. One of these deceitful mechanisms is the ability to survive inside host cells,[3] which can lead to recurring infections that are recalcitrant to treatment with most antibiotics.[4] For example, vancomycin, an antibiotic of last resort for MRSA infections, is unable to eradicate intracellular MRSA as the antibiotic is unable to sufficiently accumulate inside infected host cells. This has led to clinical failure, particularly for pneumonia-induced MRSA, in more than 40% of cases treated with a standard vancomycin dosing regimen.[5]

Arylthiazoles represent a new promising class of antibiotics that are effective against an array of clinically-relevant strains of MRSA.[1, 6–13] Several structural modifications have been made to improve both the antibacterial activity and the drug-likeness of the first discovered arylthiazole **1a** (Figure 1).[1] Briefly, the biphenyl and naphthyl analogues **1b** and **1c** demonstrated better anti-MRSA potency,[1] while incorporating the Schiff's (C=N) bond within a pyrimidine ring enhanced the metabolic stability, but, at the same time, significantly deteriorated the aqueous solubility (compound **1d** aqueous solubility limit = 2.2 μg/mL, Figure 1). In order to improve the water solubility, the pyrimidine linker was replaced with an oxadiazole that has fewer carbons and a larger polar surface area.[14] Though the oxadiazole-containing phenylthiazoles exhibited a 50 to 65-fold improvement in aqueous solubility and high metabolic stability, their anti-MRSA activity, in general, was less potent than the corresponding pyrimidine-containing analogues (Figure 1). In this regard, the MIC value of the most potent oxadiazole analogue was three-times less active than the pyrimidine analogue (Figure 1). More importantly, the oxadiazole-containing analogues lost one unique advantage over vancomycin, their rapid bactericidal activity against MRSA.[8] The overall result was none of the previously synthesized phenylthiazoles were able to reach the intracellular niches where MRSA harbors in a sufficient concentration either due to poor solubility/permeability, moderate antibacterial effect and/or slow bactericidal mode of action (Figure 1S for 1st generation phenylthiazoles & Figure 2S for 2nd generation phenylthiazoles).

In the present work, finer tuning of the linker hetero-ring, since it has a significant impact on both metabolic stability and physicochemical properties, has been applied in order to keep the metabolic stability, aqueous solubility and enhance antibacterial efficacy. Replacing the oxadiazole linker with a second thiazole ring, as discussed in the present work, achieved the desired result. Therefore, the present study addresses three objectives: to examine the anti-MRSA activity of the new series of arylthiazoles, to investigate their capability to penetrate and eradicate intracellular MRSA, and to confirm the potent anti-MRSA activity in a

Caenorhabditis elegans animal model. In addition, the antibacterial mode of action of the new arylthiazole analogues has been confirmed.

2. RESULTS AND DISCUSSION

2.1. CHEMISTRY

The lipophilic tail of the lead compound **1a** consists of *p*-*n*-butylphenyl group (Figure 1). This moiety was chosen to construct the lipophilic part of the new series, in addition to the biphenyl and 2-naphthyl moieties that were previously proven to enhance anti-MRSA activity.[1] The three methylketones **2a-c** were prepared from the corresponding thioamide, as reported elsewhere.[1] Bromination of **2a-c** using a standard bromine/glacial acetic acid protocol, followed by reaction with thiourea, thiosemicarbazide or amidinothiourea afforded the final products **4a-i** (Scheme 1).

2.2. BIOLOGICAL RESULTS AND DISCUSSION

Using our previously defined structure-activity-relationships (SAR),[14, 15] amino, hydrazinyl and guanidinyl moieties were selected as the cationic part and connected to the thiazole linker to build a small focused library of nine final products **4a-4i**. The minimum inhibitory concentration (MIC) and the minimum bactericidal concentration (MBC) of these final products, in addition to linezolid, and vancomycin were determined using the broth microdilution method (Table 1).

Among all tested compounds, the aminothiazoles **4a-4c** appeared to be ineffective, and the anti-MRSA activity improved by increasing the number of nitrogen atoms present in the cationic head, as previously identified with oxadiazole-containing derivatives.[14] Hence, the guanidine-containing derivatives **4g-4i** demonstrated lower MIC values than their corresponding amine or hydrazine analogues (Table 1). The naphthyl derivative **4i** showed antimicrobial potency comparable with two drugs of choices commonly used in treatment of invasive MRSA infections (vancomycin and linezolid). Of note, compound **4i** maintained its potency against two *S. aureus* strains exhibiting high-level resistance to vancomycin (VRSA4 and VRSA10). Furthermore, similar to the previous generations of phenylthiazoles, **4i** appears to be bactericidal as its MBC values matched or were two-fold higher than its MIC values against both MRSA and VRSA (Table 1). This observation was confirmed using a standard time-kill assay against MRSA USA400, an invasive strain of community-associated MRSA that is a significant source of infection in North America[16] (Figure 2). Compound **4i** retained its unique feature as a rapid bactericidal agent, compared to vancomycin, as it completely eliminated MRSA cells within four hours, while vancomycin required 24 hours to achieve the same effect (Figure 2), while the corresponding oxadiazole analogue behaves like vancomycin in its slow bactericidal action against MRSA.×.[14] The rapid killing kinetics of **4i** is posited to be beneficial in helping to resolve an infection more rapidly and to limit the emergence of rapid resistance to the arylthiazoles.[17]

As **4i** demonstrated consistent MIC values against a panel of clinically-relevant MRSA isolates, which are highly comparable to the two cornerstone antibiotics for treatment of invasive MRSA infections (vancomycin and linezolid), and exhibited rapid killing kinetics,

we moved to investigate safety and the ability of **4i** to penetrate and target MRSA harbouring inside host immune cells, namely macrophages. Before moving to the intracellular assay, the cytotoxic effect of compound **4i** was tested against HaCaT cells. Figure 3 indicated that **4i** is not toxic up to 32 μg/mL. This represents a 4-to-16 fold difference between the MIC values obtained for **4i** against MRSA.

Initially, the cytotoxic effect of **4i** on murine macrophage (J774) cells was examined. Compound **4i** was found to be non-toxic up to 16 μg/mL (Figure 4A). Thus, this concentration was utilized to treat macrophage cells that were infected with MRSA USA400. As depicted in Figure 4B, after four hours (same time required to eradicate a high inoculum of extracellular MRSA; Figure 2), **4i** is unable to reduce MRSA CFU/mL when compared to untreated samples. However, after 24-hours of treatment, an 81% reduction of MRSA CFU in infected macrophages is observed indicating **4i** accumulates at a concentration sufficient to kill MRSA inside macrophages. Vancomycin, as expected, was not able to reduce the presence of MRSA inside infected J774 cells, even after 24 hours of treatment. Mindful of these results, it appears naphthylthiazole **4i** (at 16 μg/mL) has the ability to gain entry into macrophage cells and to significantly reduce the burden of MRSA inside infected macrophages.

The promising result obtained from the intracellular infection experiment led us to confirm the anti-MRSA activity of **4i** in a *Caenorhabditis elegans* (*C. elegans*) animal model. *C. elegans* was first infected with the highly pathogenic MRSA USA300 strain, and then treated with compound **4i**, lead compound **1c** or vancomycin (Figure 5). Compound **4i** retained its potent anti-MRSA activity *in vivo* and reduced the burden of MRSA USA300 by approximately 30%. This value is three times better than both the lead compound **1c** and vancomycin, under the same experimental conditions, as depicted in Figure 5. The low reduction of MRSA CFU observed with vancomycin may be due to the concentration used (20 μg/mL) and the duration of treatment. In humans, the peak serum concentration of vancomycin is 40 mg/L. This is twice the concentration used in the *C. elegans* experiment which we suspect is one reason why a larger reduction in MRSA CFU/mL was not observed. Additionally, as noted in the time-kill assay, vancomycin exhibits slow bactericidal activity requiring 24 hours to completely eradicate a high inoculum of MRSA. In the *C. elegans* experiment, the duration of treatment employed was 18 hours, which may have contributed to the limited reduction in MRSA CFU in infected worms treated with vancomycin.

After confirming the extra- and intracellular antibacterial activity of compound **4i** using *in vitro* and *in vivo* models, we moved next to confirm the antibacterial mode of action. Recently, in-depth examination of the mechanism of action of the lead compound **1a** revealed this compound exerts its effect by inhibiting bacterial cell wall synthesis. Previously, close inspection of the SAR around the aminoguanidine of **1a** revealed a nitrogenous-bearing group was essential for the compound's potent anti-MRSA activity. Given this particular functional group was modified in **4i**, we were compelled to confirm that the modification made did not alter the antibacterial mode of action of this compound. In order to confirm **4i** exerts its antibacterial effect by inhibiting bacterial cell wall synthesis, we analyzed the presence of the last soluble precursor of peptidoglycan (a major component of the bacterial cell wall) synthesis in the cytoplasm of *S. aureus* cells treated with either **4i**

or vancomycin (an agent known to inhibit bacterial cell wall synthesis). This precursor, UDP-*N*-acetylmuramyl pentapeptide, will accumulate inside cells exposed to cell wall active antibiotics. *S. aureus* lysate treated with **4i** or vancomycin was analyzed using HPLC/MS and the peak corresponding to UDP-*N*-acetylmuramyl pentapeptide was monitored (Figure 6). Compound **4i** and vancomycin both generated a noticeable increase in the peak that corresponded to UDP-*N*-acetylmuramyl pentapeptide supporting the hypothesis that **4i** does inhibit bacterial cell wall synthesis (Figure 6). Though exposure of *S. aureus* to **4i** led to a smaller increase in the peak intensity relative to vancomycin, we suspect this was due in part to lysis of some cells at the high concentration (10 ×MIC) used (thus leading to loss/release of the pentatpeptide molecule from these cells). Mass spectrometry confirmed the peak corresponded to the same mass-to-charge ratio (*m/z*) for the pentapeptide (*m/z* = 1150.3588).

To confirm that bacterial cell wall synthesis is the main target of compound **4i**, we investigated the mode of action using Bacterial Cytological Profiling (BCP) - a rapid and precise approach for identifying the likely cellular pathway affected by an antibacterial agent.[18] BCP has not yet been developed for *S. aureus* but is well-established for another Gram-positive bacterial pathogen, *Bacillus subtilis*. Thus we investigated the mechanism of action of compound **4i** using *B. subtilis* (MIC = 1 μg/mL). *B. subtilis* cells treated with **4i** at 5 × MIC lysed after two hours of exposure confirming the compound's rapid bactericidal activity. When cells were treated with a slightly lower concentration of 4 × MIC in media containing the osmotic stabilizing agent MSM (magnesium sucrose maleic acid), they became misshapen and formed small bulges after two hours in the presence of methylsulfonylmethane (Figure 7D and 7P). These results were compared with cells treated with known cell wall active compounds, such as D-cyloserine (Figure 7N) and oxacillin (Figure 7F), which also led to large bulges and misshapen cells (Figure 7F). Cell shape defects and cell lysis are hallmark characteristics of compounds that target the cell wall, confirming that **4i** exerts its rapid bactericidal effect mainly *via* inhibition of cell wall biogenesis.

The final step in our analysis of **4i** involved examining how the structural modification made would impact its stability to hepatic metabolism, a crucial factor that impacts the size and frequency of dose administered to patients afflicted with a MRSA infection. Compound **4i** is superior to the lead compound **1a** as it is cleared by human liver micrsomes at a much lower rate than **1a** (Table 2). The half-life of **4i** exceeds two hours indicating the compound is metabolized at a moderate rate. The clearance rate decreased and the half-life increased significantly for compound **4i** in the absence of NADPH, indicating this compound is most likely metabolized by the cytochrome-P450 system in the liver (Table 2).

3. CONCLUSION

In conclusion, incorporating the C=N of phenylthiazoles within a thiazole ring generated a prologue for a new series of anti-MRSA antibacterial agents with balanced PD/PK properties. Using previously identified active substituents, the SAR at the lipophilic tail and cationic part were explored and compound **4i** with 2-naphtyl moiety from one side and a guanidine cationic head was found to be the most active member in this new set. The

naphtylthiazole **4i** retained the rapid bactericidal properties of first-generation derivatives, in addition to enhanced liver metabolic stability, and a unique ability to target intracellular MRSA.

4. EXPERIMENTAL SECTION

4.1. CHEMISTRY

4.1.1. General—^{1}H NMR spectra were run at 400 MHz and ^{13}C spectra were determined at 100 MHz in deuterated dimethyl sulfoxide (DMSO-d_6) on a Varian Mercury VX-400 NMR spectrometer. Chemical shifts are given in parts per million (ppm) on the delta (δ) scale. Chemical shifts were calibrated relative to those of the solvents. Flash chromatography was performed on 230-400 mesh silica. The progress of reactions was monitored with Merck silica gel IB2-F plates (0.25 mm thickness). Mass spectra were recorded at 70 eV. High resolution mass spectra for all ionization techniques were obtained from a FinniganMAT XL95. Melting points were determined using capillary tubes with a Stuart SMP30 apparatus and are uncorrected.

4.1.2. Preparation of compounds 3a-c

General procedure: To an appropriate methylketone **2** (1.8 mmol) was dissolved in warm acetic acid (10 mL), a solution of bromine (0.546 g, 0.182 mL, 3.4 mmol) in acetic acid (10 mL) was added gradually with constant stirring. After complete addition of bromine, the reaction mixture was maintained at a temperature range between 65-75 °C for one additional hour until evolution of hydrogen bromide gas ceased. The reaction mixture was allowed to cool down to room temperature and quenched with ice/water (100 mL). The organic materials were extracted with ethyl acetate (50 mL × 3 portions), dried over anhydrous $MgSO_4$, and the solvent was evaporated under reduced pressure. The obtained crude material was then purified with a silica gel column chromatography using ethyl acetate: hexane (1:9) as an eluent. Physical properties and spectral analysis of isolated products are listed below:

4.1.2.1. 2-Bromo-1-(2-(4-butylphenyl)-4-methylthiazol-5-yl)ethan-1-one (3a): Orange oil (0.51 g, 79%); ^{1}H NMR (DMSO-d_6) δ: 7.90 (d, J = 8.4 Hz, 2H), 7.36 (d, J = 8.4 Hz, 2H), 4.46 (s, 2H), 2.63 (t, J = 5.6 Hz, 2H), 2.48 (s, 3H), 1.59 (m, 2H), 1.34 (m, 2H), 0.58 (t, J = 6 Hz, 3H). MS (*m/z*) 354 (M+2), 352 (M^+); Anal. Calc. for: ($C_{16}H_{18}BrNOS$) (M.W. = 352): C, 54.55; H, 5.15; N, 3.98%; Found: C, 58.54; H, 5.16; N, 3.96%.

4.1.2.2. 1-(2-([1,1′-Biphenyl]-4-yl)-4-methylthiazol-5-yl)-2-bromoethan-1-one (3b): Yellowish white solid (0.49 g, 80%); mp = 128 °C; ^{1}H NMR (DMSO-d_6) δ: 8.06 (d, J = 6.4 Hz, 2H), 7.84 (d, J = 6.4 Hz, 2H), 7.72 (d, J = 7.2 Hz, 2H), 7.50 (t, J = 6.8 Hz, 2H), 7.40 (t, J = 7.2 Hz, 1H), 4.45 (s, 2H), 2.73 (s, 3H); MS (*m/z*) 374 (M+2), 372 (M^+); Anal. Calc. for: ($C_{18}H_{14}BrNOS$) (M.W. = 372): C, 58.07; H, 3.79; N, 3.76%; Found: C, 58.09; H, 3.81; N, 3.77%.

4.1.2.3. 2-Bromo-1-(4-Methyl-2-(4-(naphthalen-2-yl)phenyl)thiazol-5-yl)ethan-1-one (3c): Yellowish white solid (0.55 g, 85%); mp = 132 °C; ^{1}H NMR (DMSO-d_6) δ: 8.65 (s,

1H), 8.17-8.06 (m, 4H), 7.64 (m, 2H), 4.52 (s, 2H), 2.82 (s, 3H); MS (*m/z*) 348 (M+2), 346 (M^+); Anal. Calc. for: ($C_{16}H_{12}BrNOS$) (M.W. = 346): C, 55.50; H, 3.49; N, 4.05%; Found: C, 55.52; H, 3.51; N, 4.07%.

4.1.3. Preparation of compounds 4a-i

General procedure: To a solution of bromoacetyl **3** (0.56 mmol) in absolute ethanol (5 mL), proper thiourea or thioamide (1.25-2.5 mmol) and anhydrous potassium carbonate (0.2 g, 1.4 mmol) were added. The reaction mixture was heated at reflux for 4-8 hours. After consuming all starting materials, as monitored by TLC, the reaction was quenched with cold water (50 mL). The formed flocculated solid was filtered, washed with water and purified by crystallization from absolute ethanol or via acid-base extraction using HCl (1 M, 50 mL). Upon neutralization with sodium carbonate to pH 7–8, the desired products were precipitated. Physical properties and spectral analysis of isolated products are listed below:

4.1.3.1. 2′-(4-Butylphenyl)-4′-methyl-[5,5′-bithiazol]-2-amine (4a): Yellow crystals (0.15 g, 82%) mp = 79 °C; ^{1}H NMR (DMSO-d_6) δ: 7.79 (d, *J* = 7.6 Hz, 2H), 7.28 (d, *J* = 8.4 Hz, 2H), 7.19 (brs, 2H), 6.74 (s, 1H), 2.61 (t, *J* = 7.2 Hz, 2H), 2.47 (s, 3H), 1.58 (p, *J* = 7.6 Hz, 2H), 1.34 (m, 2H), 0.9 (t, *J* = 7.2 Hz, 3H). ^{13}C NMR (DMSO-d_6) δ: 168.40, 163.15, 148.46, 144.97, 142.31, 131.24, 129.53, 129.48, 128.20, 126.15, 103.19, 35.13, 33.29, 22.23, 17.81, 14.19. MS (*m/z*) 329; HRMS (EI) m/z X M+, calcd for $C_{17}H_{19}N_3S_2$ 329.1010; Anal. Calc. for: ($C_{17}H_{19}N_3S_2$) (M.W. = 329): C, 61.97; H, 5.81; N, 12.75%; Found: C, 61.96; H, 5.82; N, 12.73%.

4.1.3.2. 2′-([1,1′-Biphenyl]-4-yl)-4′-methyl-[5,5′-bithiazol]-2-amine (4b): Yellow solid (0.15 g, 78%); mp = 128 °C; ^{1}H NMR (DMSO-d_6) δ: 7.97 (d, *J* = 8.4 Hz, 2H), 7.76 (d, *J* = 8.4 Hz, 2H), 7.71 (d, *J* = 7.2 Hz, 2H), 7.47 (t, *J* = 6.8 Hz, 2H), 7.40 (t, *J* = 7.2 Hz, 1H), 7.21 (brs, 2H), 6.78 (s,1H), 2.71 (s, 3H); ^{13}C NMR (DMSO-d_6) δ: 168.45, 162.52, 148.76, 142.20, 141.82, 139.61, 132.63, 129.52, 128.40, 127.80, 127.21, 127.07, 126.75, 103.48, 17.86; MS (*m/z*) 349; HRMS (EI) *m/z* 349.0718 M^+, calcd for $C_{19}H_{15}N_3S_2$ 349.0707; Anal. Calc. for: ($C_{19}H_{15}N_3S_2$): C, 65.30; H, 4.33; N, 12.02%; Found: C, 65.31; H, 4.34; N, 12.03%.

4.1.3.3. 4′-methyl-2′-(Naphthalen-2-yl)-[5,5′-bithiazol]-2-amine (4c): Yellow solid (0.15 g, 80%). mp = 142 °C; ^{1}H NMR (DMSO-d_6) δ: 8.49 (s, 1H), 8.09-7.99 (m, 4H), 7.60 (m, 2H), 6.99 (s, 1H), 6.98 (brs, 2H), 2.75 (s, 3H); ^{13}C NMR (DMSO-d_6) δ: 168.90, 162.15, 160.73, 157.52, 148.78, 141.56, 133.95, 133.39, 130.97, 129.24, 128.98, 128.18, 127.57, 127.44, 125.41, 123.77, 17.81; MS (*m/z*) 323; HRMS (EI) *m/z* 323.0558 M^+, calcd for $C_{17}H_{13}N_3S_2$ 323.0551; Anal. Calc. for: ($C_{17}H_{13}N_3S_2$): C, 63.13; H, 4.05; N, 12.99%; Found: C, 63.15; H, 4.06; N, 12.99%.

4.1.3.4. 2-(4-Butylphenyl)-2′-hydrazinyl-4-methyl-5,5′-bithiazole (4d): Brownish solid (0.17 g, 88%) mp = 110 °C; ^{1}H NMR (DMSO-d_6) δ: 9.21 (brs, 1H), 7.92 (s, 1H), 7.83 (d, *J* = 8.4 Hz, 2H), 7.30 (d, *J* = 8 Hz, 2H), 4.05 (brs, 2H), 2.61 (t, *J* = 7.2 Hz, 2H), 2.47 (s, 3H), 1.58 (p, *J* = 7.2 Hz, 2H), 1.34 (m, 2H), 0.9 (t, *J* = 7.2 Hz, 3H); ^{13}C NMR (DMSO-d_6) δ: 169.58, 164.38, 155.25, 149.72, 147.34, 145.36, 131.00, 129.56, 126.32, 115.97, 35.07,

33.28, 22.18, 17.67, 14.20; MS (*m/z*) 344; HRMS (EI) *m/z* 344.1115 M^+, calcd for $C_{17}H_{20}N_4S_2$ 344.1129; Anal. Calc. for: ($C_{17}H_{20}N_4S_2$) (M.W. = 344): C, 59.27; H, 5.85; N, 16.26%; Found: C, 59.28; H, 5.83; N, 16.28%.

4.1.3.5. 2-([1,1′-Biphenyl]-4-yl)-2′-hydrazinyl-4-methyl-5,5′-bithiazole (4e): Yellow solid (0.17 g, 94%). mp = 128 °C; ^{1}H NMR (DMSO-d_6) δ: 8.74 (brs, 1H), 7.99 (d, *J* = 6.8 Hz, 2H), 7.76 (d, *J* = 6.8 Hz, 2H), 7.75 (d, *J* = 6.8 Hz, 2H), 7.48 (t, *J* = 6.8 Hz, 2H), 7.36 (t, *J* = 6.4 Hz, 1H), 7.21 (brs, 2H), 6.86 (s,1H), 2.66 (s, 3H); ^{13}C NMR (DMSO-d_6) δ: 168.43, 162.48, 148.73, 142.23, 141.79, 139.60, 132.39, 129.52, 129.44, 127.98, 127.79, 127.07, 126.74, 103.49, 17.85; MS (*m/z*) 364; HRMS (EI) *m/z* 364.0799 M^+, calcd for $C_{19}H_{16}N_4S_2$ 364.0816; Anal. Calc. for: ($C_{19}H_{16}N_4S_2$): C, 62.61; H, 4.42; N, 15.37%; Found: C, 62.63; H, 4.43; N, 15.38%.

4.1.3.6. 2′-Hydrazinyl-4-methyl-2-(naphthalen-2-yl)-5,5′-bithiazole (4f): Yellowish solid (0.17 g, 87%). mp = 139 °C; ^{1}H NMR (DMSO-d_6) δ: 8.74 (brs, 1H), 8.52 (s, 1H), 8.08-7.98 (m, 4H), 7.61 (m, 2H), 7.21 (brs, 2H), 6.98 (s, 1H), 2.74 (s, 3H); ^{13}C NMR (DMSO-d_6) δ: 169.00, 162.13, 161.03, 157.57, 148.58, 141.66, 133.96, 133.33, 130.87, 129.44, 128.97, 128.27, 127.56, 127.42, 125.39, 123.67, 17.80; MS (*m/z*) 338; Anal. Calc. for: ($C_{17}H_{14}N_4S_2$) (M.W. = 338): C, 60.33; H, 4.17; N, 16.55%; Found: C, 60.34; H, 4.18; N, 16.57%.

4.1.3.7. 1-(2′-([4-Buylphenyl)-4′-methyl-[5,5′-bithiazol]-2-yl)guanidine (4g): Yellowish brown solid (0.18 g, 87%); mp = 118 °C; ^{1}H NMR (DMSO-d_6) δ: 7.87 (brs, 1H), 7.85 (brs, 1H), 7.79 (d, *J* = 8.4 Hz, 2H), 7.27 (d, *J* = 8.0 Hz, 2H), 6.95 (brs, 2H), 6.88 (s, 1H), 2.61 (t, *J* = 7.2 Hz, 2H), 2.47 (s, 3H), 1.58 (p, *J* = 7.2 Hz, 2H), 1.34 (m, 2H), 0.90 (t, *J* = 7.2 Hz, 3H); ^{13}C NMR (DMSO-d_6) δ: 168.41, 163.15, 157.15, 147.96, 145.07, 143.31, 131.26, 129.73, 128.52, 126.15, 104.19, 35.13, 33.29, 22.23, 17.91, 14.29; MS (*m/z*) 371; HRMS (EI) *m/z* 371.1233 M^+, calcd. For $C_{18}H_{21}N_5S_2$ 371.1238; Anal. Calc. for: ($C_{18}H_{21}N_5S_2$): C, 58.19; H, 5.70; N, 18.85%; Found: C, 58.18; H, 5.70; N, 18.85%.

4.1.3.8. 1-(2′-([1,1′-Biphenyl]-4-yl)-4′-methyl-[5,5′-bithiazol]-2-yl)guanidine (4h): Yellow solid (0.18 g, 82%). mp = 128 °C; ^{1}H NMR (DMSO-d_6) δ: 7.98 (d, *J* = 6.8 Hz, 2H), 7.78 (d, *J* = 6.8 Hz, 2H), 7.72 (d, *J* = 6.8 Hz, 2H), 7.47 (t, *J* = 7.6 Hz, 2H), 7.40 (t, *J* = 7.2 Hz, 1H), 7.21 (brs, 4H), 6.94 (s,1H), 2.60 (s, 3H); ^{13}C NMR (DMSO-d_6) δ: 168.55, 162.47, 157.61, 148.70, 141.86, 141.53, 139.58, 132.57, 129.51, 128.40, 127.80, 127.22, 127.08, 126.78, 105.37, 17.85; MS (*m/z*) 391; HRMS (EI) *m/z* 391.0929 M^+, calcd for $C_{20}H_{17}N_5S_2$ 391.0925; Anal. Calc. for: ($C_{20}H_{17}N_5S_2$): C, 61.36; H, 4.38; N, 17.89%; Found: C, 61.37; H, 4.39; N, 17.94%.

4.1.3.9. 1-(4′-Methyl-2′-(naphthalen-2-yl)-[5,5′-bithiazol]-2-yl)guanidine (4i): Yellowish red solid (0.17 g, 82%); mp = 145 °C; ^{1}H NMR (DMSO-d_6) δ: 8.51 (s, 1H), 8.10-7.94 (m, 4H), 7.60 (m, 2H), 6.88 (s, 1H), 6.78 (brs, 4H), 2.60 (s, 3H); ^{13}C NMR (DMSO-d_6) δ: 167.77, 165.19, 152.83, 140.97, 134.11, 133.33, 130.62, 129.34, 129.27, 129.08, 128.18, 127.74, 127.47, 125.79, 124.67, 123.85, 123.78, 17.74; MS (*m/z*) 365; HRMS (EI) *m/z* 365.0777 M^+, calcd for $C_{18}H_{15}N_5S_2$ 365.0769; Anal. Calc. for: ($C_{18}H_{15}N_5S_2$): C, 59.16; H, 4.14; N, 19.16%; Found: C, 59.18; H, 4.15; N, 19.17%.

4.2. ANTIMICROBIAL TESTING

4.2.1. Determination of Minimum Inhibitory Concentration (MIC) and Minimum Bactericidal Concentration (MBC)—Clinical isolates of *S. aureus* were obtained through the Network of Antimicrobial Resistance in *Staphylococcus aureus* (NARSA) program and BEI Resources.

The MICs of the newly synthesized compounds, tested against isolates of *S. aureus*, were determined using the broth microdilution method in accordance with the Clinical and Laboratory Standards Institute.[19] Bacteria were cultured in cation-adjusted Mueller Hinton broth in a 96-well plate. Compounds, using triplicate samples, were added to the plate and serially diluted. Plates were incubated at 37 °C for 20 hours prior to determining the MIC. Plates were visually inspected and the MIC was categorized as the concentration at which no visible growth of bacteria was observed. The average of triplicate MIC determinations is reported. The MBC was determined by transferring a small aliquot (5 uL), from wells where no growth was observed (in the MIC plates), onto Tryptic soy agar plates. Plates were incubated at 37 °C for at least 18 hours prior to determining the MBC; the MBC was categorized as the lowest concentration where 99.9% of bacterial growth was inhibited.

4.2.2. Time-kill assay—MRSA USA400 cells in logarithmic growth phase (OD_{600} > 0.800) were diluted to ~ 10^6 colony-forming units (CFU/mL) and exposed to concentrations equivalent to 4 × MIC (in triplicate) of **4i** and vancomycin in Tryptic soy broth. Aliquots (100 μL) were collected from each treatment after 0, 2, 4, 6, 8, 10, 12, and 24 hours of incubation at 37 °C and subsequently serially diluted in phosphate-buffered saline (PBS). Bacteria were then transferred to Tryptic soy agar plates and incubated at 37 °C for 18-20 hours before viable CFU/mL was determined.

4.2.3. Intracellular infection of J774 cells with MRSA and treatment with compound 4i

Toxicity assessment: Compound **4i** was assayed (at concentrations of 8, 16, 32, and 64 μg/mL) against a murine macrophage (J774) cell line to determine the potential toxic effect *in vitro*. Briefly, cells were cultured in Dulbecco's Modified Eagle Medium (DMEM) supplemented with 10% FBS at 37 °C with CO_2 (5%). Control cells received DMSO alone at a concentration equal to that in drug-treated cell samples. The cells were incubated with the compounds (in triplicate) in a 96-well plate at 37 °C with CO_2 (5%) for two hours. The assay reagent MTS 3-(4,5-dimethylthiazol-2-yl)-5-(3-carboxymethoxyphenyl)-2-(4-sulfophenyl)-2*H*-tetrazolium) (Promega, Madison, WI, USA) was subsequently added and the plate was incubated for four hours. Absorbance readings (at OD_{490}) were taken using a kinetic microplate reader (Molecular Devices, Sunnyvale, CA, USA). The quantity of viable cells after treatment with each compound was expressed as a percentage of the viability of DMSO-treated control cells (average of triplicate wells ± standard deviation). The toxicity data was analyzed via a one-way ANOVA, with post hoc Dunnet's multiple comparisons test ($P < 0.05$), utilizing GraphPad Prism 6.0 (GraphPad Software, La Jolla, CA).

4.2.4. Eradication of intracellular MRSA—Murine macrophage cells (J774) were cultured in Dulbecco's Modified Eagle Medium (DMEM) supplemented with 10% FBS at

37 °C with CO_2 (5%). J774 cells were exposed to MRSA USA400 cells at a multiplicity of infection of approximately 100:1. One-hour post-infection, J774 cells were washed with gentamicin (50 μg/mL) to kill extracellular MRSA. Compound **4i** and vancomycin, at a concentration equal to 16 μg/mL, were added, in triplicate. At specified time points (4, 8, 12, and 24 hours), the test agents were removed; J774 cells were washed with gentamicin (50 μg/mL) and subsequently lysed using 0.1% Triton-X 100. The solution was serially diluted in PBS and transferred to Tryptic soy agar plates in order to enumerate the viable number of MRSA colony-forming units (CFU) present inside J774 cells. Plates were incubated at 37°C for 18-22 hours before counting viable CFU/mL. Data are presented as percent reduction of MRSA CFU/mL in infected J774 cells in relation to the untreated control. The data was analyzed via a t-test ($P < 0.05$), utilizing GraphPad Prism 6.0 (GraphPad Software, La Jolla, CA). Asterisks (*) indicate statistical significance between compound **4i** and vancomycin.

4.2.5. *In vivo* examination of 1c, 4i and vancomycin to kill MRSA USA300 in a *Caenorhabditis elegans* model—To examine the efficacy of the thiazole compounds to treat a MRSA infection *in vivo*, the whole animal model *Caenorhabditis elegans* (*C. elegans*) was utilized. The temperature-sensitive sterile mutant strain *C. elegans* AU37 [sek-1(km4); glp-4(bn2) I] was used as this strain is sterile at room temperature and capable of laying eggs only at 15°C. Additionally, this strain is more susceptible to infection due to a mutation in the *sek-1* gene of the p38 mitogen-activated protein kinase pathway. Briefly, worms were grown for five days at 15°C (permitting worms to lay eggs) on nematode growth medium (NGM) agar plates seeded with a lawn of *Escherichia coli* (*E. coli*) OP50. The eggs were harvested by bleaching and maintained for 24 hours at room temperature with gentle agitation for hatching. Hatched larvae were transferred to a new NGM plate seeded with *E. coli* OP50 and were kept at room temperature for 4-5 days until worms reached the adult stage of growth (L4). Adult worms were collected and washed three times with PBS in a 1:10 ratio to remove *E. coli*.

To test the antibacterial activity of the compounds and vancomycin against MRSA *in vivo*, adult worms were transferred to TSA agar plates seeded with a lawn of MRSA USA300 (highly pathogenic to *C. elegans*) for infection. After six hours of infection, worms were collected and washed with M9 buffer three times before transferring 25-30 worms to wells in a 96-well microtiter plate. Worms were incubated with 20 μg/mL of tested compounds, vancomycin (positive control), or PBS (negative control) (in triplicate). After treatment for 18 hours, worms were washed three times with M9 buffer and then examined microscopically to examine morphological changes and viability. They were subsequently lysed in microcentrifuge tubes containing 200 mg of 1.0-mm silicon carbide particles (Biospec Products, Bartlesville, OK) that were vortexed for one minute. Samples were serially diluted and plated onto TSA plates containing 5 μg/mL nalidixic acid to select for MRSA growth. Plates were incubated at 37°C for 17 hours before viable CFU was determined. MRSA USA300 CFU was divided by the number of worms receiving each treatment and the percent reduction in MRSA USA300 growth, relative to PBS-treated worms, was subsequently calculated.

4.2.6. Mechanism of action study for compound 4i against *S. aureus*—To determine if **4i** exhibits its effect on staphylococci by inhibiting cell wall synthesis, the accumulation of the final soluble cell wall precursor inside bacterial cells (UDP-*N*-acetylmuramyl pentapeptide) was detected using the procedure described in a previous study,[20] with the following modifications. *S. aureus* NRS107 (RN4220), in early logarithmic growth stage (OD_{600} ~ 0.60), was incubated with 130 μg/mL chloramphenicol for 15 minutes at 37 °C. Bacteria were subsequently incubated with either 10 × MIC of compound **4i** or vancomycin (positive control) for 30 minutes at 37 °C. Untreated samples served as a negative control. Samples were next centrifuged at 10,000 rpm, the supernatant discarded, and pellet re-suspended in 1 mL of sterile deionzined water. The bacterial pellet was boiled at 100°C for 30 minutes before samples were chilled on ice for 10 minutes. UDP-*N*-acetylmuramyl-pentapeptide was measured using an Agilent High Performance Liquid Chromatography coupled to a time-of-flight Mass Spectrometer (HPLC-MS). A Waters XBridge Phenyl (2.1 × 100 mm, 3.5 um) chromatography column was used, with mobile phases of water, 0.1% formic acid (Buffer A) and acetonitrile, 0.1% formic acid (Buffer B). A gradient of 5-20% Buffer B over 14 minutes was used, with a flow rate of 0.3 mL/min. An electrospray source was used, in positive ionization mode. Extracted Ion Chromatograms (EIC) were generated at *m/z* of 1150.3588 (20 ppm window). Mass error for UDP-*N*-acetylmuramyl-pentapeptide was <2 ppm.

4.2.7. Bacterial Cytological Profiling of Compound 4i against *Bacillus subtilis*—Cells were grown in Luria Bertani (LB) medium at 37°C (*B. subtilis*) until the optical density at 600 nm (OD_{600}) was ~0.2. Cells were then left untreated, treated with compounds, or treated with compounds in the presence of the osmotic stabilizing agent MSM (magnesium sucrose maleic acid), (*B. subtilis*) as described previously.[18, 21, 22] After two hours, cells were stained with FM 4−64 (1 μg/mL) to visualize the membranes; DAPI (1 μg/ml *B. subtilis*) to visualize the DNA, and SYTOX Green (1 μg/mL), a vital stain which is normally excluded from cells with an intact membrane but brightly stains cells that are lysed.[18] Images were collected using a Delta Vision Spectris Deconvolution microscope, as described previously.[18]

4.2.8. *In vitro* cytotoxicity analysis of compound 4i against HRT-18 cells—Compound **4i** was assayed (at concentrations of 8, 16, 32, and 64 μg/mL) against a human keratinocyte (HaCaT) cell line to determine the potential toxic effect to mammalian cells *in vitro*. Briefly, cells were cultured in Dulbecco's Modified Eagle Medium (DMEM) supplemented with 10% fetal bovine serum (FBS) at 37 °C with CO_2 (5%). Control cells received DMSO alone at a concentration equal to that in drug-treated cell samples. The cells were incubated with the compounds (in triplicate) in a 96-well plate at 37 °C with CO_2 (5%) for two hours. The assay reagent MTS 3-(4,5-dimethylthiazol-2-yl)-5-(3-carboxymethoxyphenyl)-2-(4-sulfophenyl)-2*H*-tetrazolium) (Promega, Madison, WI, USA) was subsequently added and the plate was incubated for four hours. Absorbance readings (at OD_{490}) were taken using a kinetic microplate reader (Molecular Devices, Sunnyvale, CA, USA). The quantity of viable cells after treatment with each compound was expressed as a percentage of the viability of DMSO-treated control cells (average of triplicate wells ± standard deviation). The toxicity data was analyzed via a two-way ANOVA, with post hoc

Dunnet's multiple comparisons test ($P < 0.05$), utilizing GraphPad Prism 6.0 (GraphPad Software, La Jolla, CA).

4.2.9. Examining phenylthiazole compounds' ability to re-sensitize vancomycin-resistant *S. aureus* (VRSA) to the effect of vancomycin—Tryptic soy broth was inoculated with VRS10 (5×10^5 CFU/mL), as described in a previous study.[8] Aliquots (5 mL) of the bacterial suspension were divided into microcentrifuge tubes and tested compounds (at ½ × MIC) were introduced into each tube. After sitting at room temperature for 30 minutes, samples (1 mL) from each tube were transferred to a new centrifuge tube prior to addition of a subinhibitory concentration of either vancomycin (at a concentration equivalent to 128 μg/mL). Using a 96-well microtiter plate, rows 2-8 were filled with the remaining 4 mL bacterial suspension (containing the compound). 200-μL aliquots from tubes containing both the compound and vancomycin were transferred to row 1 of the 96-well plate. After aspirating contents in the first row 4-6 times, 100 μL was transferred from wells in row 1 to row 2. This process was repeated to dilute the remaining wells containing no antibiotic. Untreated bacteria served as a control. The plate was incubated at 37 °C for 20-22 hours before the MIC was recorded. The MIC was categorized as the concentration at which no visible growth of bacteria was observed in a particular well. A fold reduction was calculated by comparing the MIC of vancomycin alone compared to the MIC of the antibiotic given in combination with each compound.

4.3. Pharmacokinetic assays

4.3.1. Human Microsomal Stability Analysis—The tested compound was incubated in duplicate with human liver microsomes at 37 °C. The reaction contained microsomal protein in 100 mM potassium phosphate, 2 mM NADPH, 3 mM $MgCl_2$, pH 7.4. A control was run for each test agent omitting NADPH to detect NADPH-free degradation. At 0, 10, 20, 40, and 60 min, an aliquot was removed from each experimental and control reaction and mixed with an equal volume of ice-cold Stop Solution (methanol containing haloperidol, diclofenac, or other internal standard). Stopped reactions were incubated at least ten minutes at −20 °C, and an additional volume of water was added. The samples were centrifuged to remove precipitated protein, and the supernatants were analyzed by LC/MS/MS to quantitate the remaining parent. Data were converted to % remaining by dividing by the time zero concentration value. Data were then fit to a first-order decay model in order to determine the half-life. Intrinsic clearance values were calculated from the half-life and the protein concentrations using the following equation: $CL_{int} = \ln(2) / (T_{1/2}$ [microsomal protein]).

Supplementary Material

Refer to Web version on PubMed Central for supplementary material.

Acknowledgments

This work was supported by Science & Technology Development Funds (STDF), Grant#5503. This work was also supported by the National Institute of Allergy and Infectious Diseases of the National Institutes of Health under Award Number R01AI130186 to M. N. S.

ABBREVIATIONS

CFU	colony forming unit
HRT-18	human colorectal cells
MSM	magnesium sucrose maleic acid

References

1. Mohammad H, Mayhoub AS, Ghafoor A, Soofi M, Alajlouni RA, Cushman M, Seleem MN. Discovery and Characterization of Potent Thiazoles versus Methicillin- and Vancomycin-Resistant *Staphylococcus aureus*. J Med Chem. 2014; 57:1609–1615. [PubMed: 24387054]
2. Centers for Disease Control and Prevention. Antibiotic Resistance Threats in the United States. 2013; 2013
3. Nguyen HM, Graber CJ. Limitations of Antibiotic Options for Invasive Infections Caused by Methicillin-Resistant *Staphylococcus aureus*: Is Combination Therapy The Answer? J Antimicrob Chemther. 2010; 65:24–36.
4. Krut O, Sommer H, Kronke M. Antibiotic-Induced Persistence of Cytotoxic *Staphylococcus aureus* in Non-Phagocytic cells. J Antimicrob Chemther. 2004; 53:167–173.
5. Moise-Broder PA, Forrest A, Birmingham MC, Schentag JJ. Pharmacodynamics of Vancomycin and Other Antimicrobials in Patients with *Staphylococcus aureus* Lower Respiratory Tract Infections. Clin Pharmacokinet. 2004; 43:925–942. [PubMed: 15509186]
6. Sashidhara KV, Rao KB, Kushwaha P, Modukuri RK, Singh P, Soni I, Shukla PK, Chopra S, Pasupuleti M. Novel Chalcone-Thiazole Hybrids as Potent Inhibitors of Drug Resistant *Staphylococcus aureus*. ACS Med Chem Lett. 2015; 6:809–813. [PubMed: 26191371]
7. Hagras M, Mohammad H, Mandour MS, Hegazy YA, Ghiaty A, Seleem MN, Mayhoub AS. Investigating the Antibacterial Activity of Biphenylthiazoles against Methicillin-and Vancomycin-Resistant *Staphylococcus aureus* (MRSA and VRSA). J Med Chem. 2017; 60:4074–4085. [PubMed: 28436655]
8. Mohammad H, Mayhoub AS, Cushman M, Seleem MN. Anti-biofilm Activity and Synergism of Novel Thiazole Compounds With Glycopeptide Antibiotics Against Multidrug-Resistant Staphylococci. J Antibiot. 2015; 68:259–266. [PubMed: 25315757]
9. Mohammad H, Reddy PV, Monteleone D, Mayhoub AS, Cushman M, Hammac GK, Seleem MN. Antibacterial Characterization of Novel Synthetic Thiazole Compounds Against Methicillin-Resistant *Staphylococcus pseudintermedius*. PloS One. 2015; 10:e0130385. [PubMed: 26086336]
10. Mohammad H, Reddy PV, Monteleone D, Mayhoub AS, Cushman M, Seleem MN. Synthesis and Antibacterial Evaluation of a Novel Series of Synthetic Phenylthiazole Compounds Against Methicillin-Resistant *Staphylococcus aureus* (MRSA). Eur J Med Chem. 2015; 94:306–316. [PubMed: 25771109]
11. Mohammad H, Younis W, Chen L, Peters CE, Pogliano J, Pogliano K, Cooper B, Zhang J, Mayhoub A, Oldfield E, Cushman M, Seleem MN. Phenylthiazole Antibacterial Agents Targeting Cell Wall Synthesis Exhibit Potent Activity in Vitro and in Vivo against Vancomycin-Resistant Enterococci. J Med Chem. 2017; 60:2425–2438. [PubMed: 28248504]
12. Seleem MA, Disouky AM, Mohammad H, Abdelghany TM, Mancy AS, Bayoumi SA, Elshafeey A, El-Morsy A, Seleem MN, Mayhoub AS. Second-Generation Phenylthiazole Antibiotics with Enhanced Pharmacokinetic Properties. J Med Chem. 2016; 59:4900–4912. [PubMed: 27187739]
13. Yahia E, Mohammad H, Abdelghany TM, Fayed E, Seleem MN, Mayhoub AS. Phenylthiazole Antibiotics: A Metabolism-Guided Approach to Overcome Short Duration of Action. Eur J Med Chem. 2017; 126:604–613. [PubMed: 27918995]
14. Hagras M, Hegazy Y, Elkabbany AH, Mohammad H, Ghaiaty A, Seleem MN, Mayhoub AS. Biphenylthiazoles with Oxadiazole Linker: An Approach to Improve the Physicochemical Properties. J Med Chem. 2016 Under reveiw.

15. Seleem MA, Disouky AM, Mohammad H, Abdelghany TM, Mancy AS, Bayoumi SA, Elshafeey A, El-Morsy A, Seleem MN, Mayhoub AS. Second-Generation Phenylthiazole Antibiotics with Enhanced Pharmacokinetic Properties. J Med Chem. 2016; 59:4900–4912. [PubMed: 27187739]
16. Van De Griend P, Herwaldt LA, Alvis B, DeMartino M, Heilmann K, Doern G, Winokur P, Vonstein DD, Diekema D. Community-Associated Methicillin-Resistant *Staphylococcus aureus*, Iowa, USA. Emerging Infect Dis. 2009; 15:1582–1589. [PubMed: 19861049]
17. Alder J, Eisenstein B. The Advantage of Bactericidal Drugs in the Treatment of Infection. Curr Infect Dis Rep. 2004; 6:251–253. [PubMed: 15265451]
18. Nonejuie P, Burkart M, Pogliano K, Pogliano J. Bacterial Cytological Profiling Rapidly Identifies The Cellular Pathways Targeted By Antibacterial Molecules. Proc Natl Acad Sci USA. 2013; 110:16169–16174. [PubMed: 24046367]
19. Clinical and Laboratory Standards Institute. Approved Standard M07-A9. Ninth. Wayne, PA: 2012. Methods for Dilution Antimicrobial Susceptibility Tests for Bacteria That Grow Aerobically.
20. Schmitt P, Wilmes M, Pugniere M, Aumelas A, Bachere E, Sahl HG, Schneider T, Destoumieux-Garzon D. Insight Into Invertebrate Defensin Mechanism of Action: Oyster Defensins Inhibit Peptidoglycan Biosynthesis by Binding to Lipid II. J Biol Chem. 2010; 285:29208–29216. [PubMed: 20605792]
21. Lamsa A, Lopez-Garrido J, Quach D, Riley EP, Pogliano J, Pogliano K. Rapid Inhibition Profiling in Bacillus Subtilis to Identify the Mechanism of Action of New Antimicrobials. ACS Chem Biol. 2016; 11:2222–2231. [PubMed: 27193499]
22. Lamsa A, Liu WT, Dorrestein PC, Pogliano K. The *Bacillus Subtilis* Cannibalism Toxin SDP Collapses The Proton Motive Force And Induces Autolysis. Mol Microbiol. 2012; 84:486–500. [PubMed: 22469514]

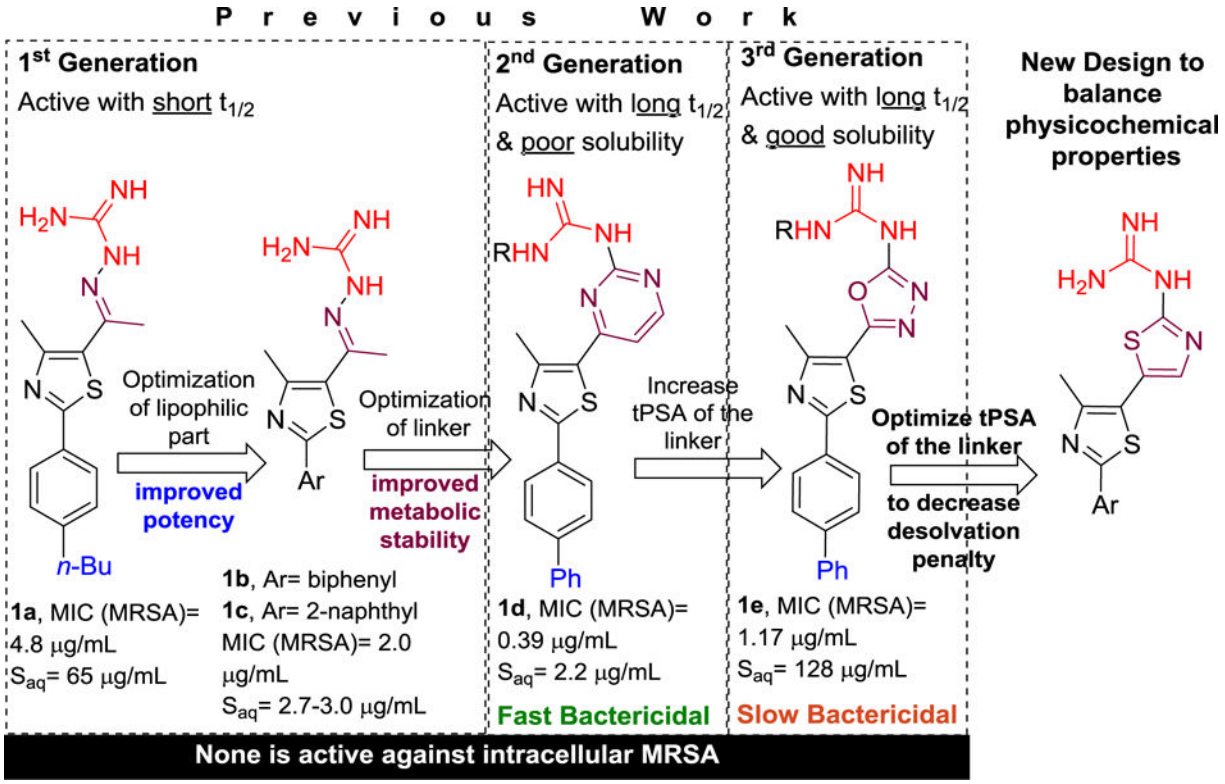

Figure 1.
Developmental progress of phenylthiazole antibiotics and the new design.

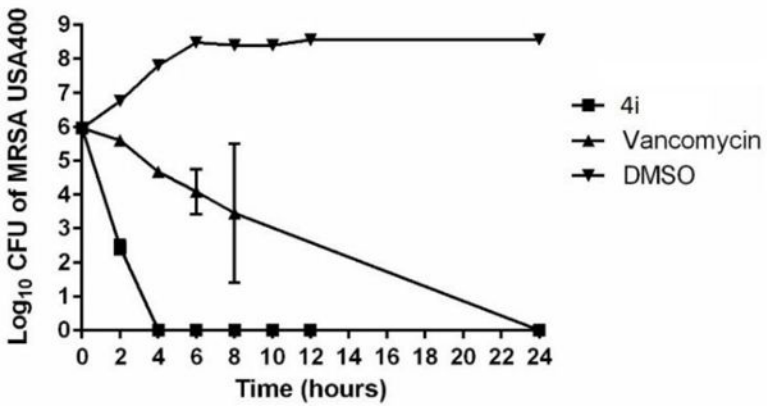

Figure 2. Time-kill analysis of thiazole compound 4i and vancomycin against methicillin-resistant *Staphylococcus aureus* (MRSA USA400) over a 24-hour incubation period at 37°C

DMSO served as a negative control. The error bars represent standard deviation values obtained from triplicate samples used for each compound/antibiotic studied.

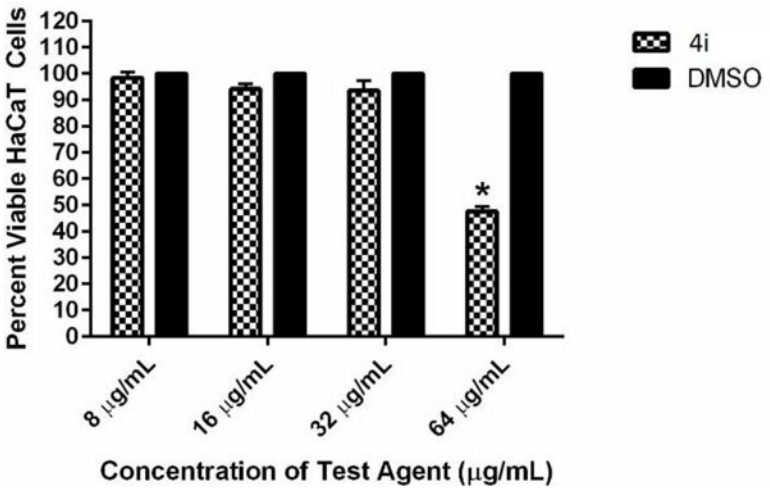

Figure 3. Toxicity analysis of compound 4i against human keratinocytes (HaCaT)

Percent viable mammalian cells (measured as average absorbance ratio (test agent relative to DMSO)) for cytotoxicity analysis of thiazole compound **4i** (tested in triplicate) at 8, 16, 32, and 64 μg/mL against HaCaT cells using the MTS 3-(4,5-dimethylthiazol-2-yl)-5-(3-carboxymethoxyphenyl)-2-(4-sulfophenyl)-2H-tetrazolium) assay. Dimethyl sulfoxide (DMSO) was used as a negative control to determine a baseline measurement for the cytotoxic impact of each compound. The absorbance values represent an average of a minimum of three samples analyzed for each compound. Error bars represent standard deviation values for the absorbance values. A two-way ANOVA, with post hoc Dunnet's multiple comparisons test, determined statistical difference between the values obtained for each compound and DMSO (denoted by the asterisk) ($P < 0.05$).

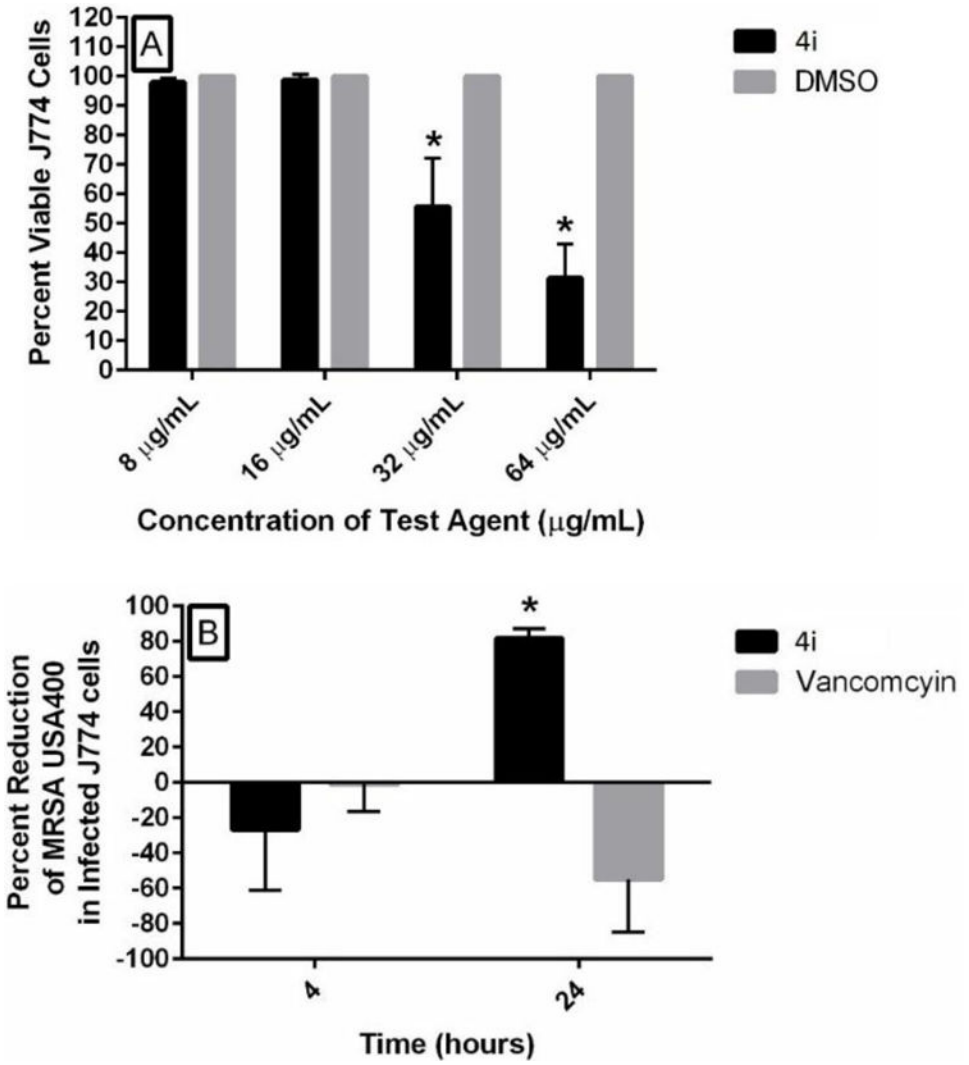

Figure 4. Toxicity analysis and examination of clearance of intracellular MRSA present in murine macrophage (J774) cells

Panel A) Percent viable mammalian cells (measured as average absorbance ratio (test agent relative to DMSO)) for cytotoxicity analysis of naphtylthiazole **4i** (tested in triplicate) at 8, 16, 32, and 64 μg/mL against J774 cells using the MTS 3-(4,5-dimethylthiazol-2-yl)-5-(3-carboxymethoxyphenyl)-2-(4-sulfophenyl)-2*H*-tetrazolium) assay. Dimethyl sulfoxide (DMSO) was used as a negative control to determine a baseline measurement for the cytotoxic impact of each compound. The absorbance values represent an average of a minimum of three samples analyzed for each compound. Error bars represent standard deviation values for the absorbance values. A one-way ANOVA, with post hoc Dunnet's multiple comparisons test, determined statistical difference between the values obtained for each compound and DMSO (denoted by the asterisk) ($P < 0.05$). **Panel B)** Percent reduction of MRSA USA400 colony forming units inside infected murine macrophage cells after treatment with 16 μg/mL of either compound **4i** or vancomycin (tested in triplicate) for 4 or 24 hours. Data were analyzed via a Student's t-test ($P < 0.05$). Asterisks (*) represent significant difference between treatment of J774 cells with **4i** in comparison to vancomycin.

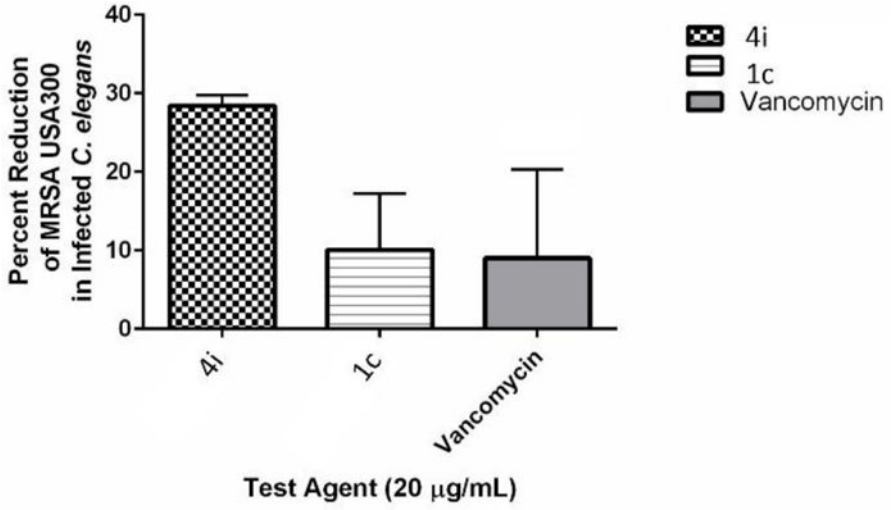

Figure 5. Antibacterial activity of 4i, 1c, and vancomycin *in vivo* against MRSA-infected *C. elegans*

In vivo examination of antibacterial activity of test agents (at 20 μg/mL) in *C. elegans* AU37 infected with methicillin-resistant *Staphylococcus aureus* USA300. Vancomycin served as a positive control. Worms (in L4 stage of growth) were infected with bacteria for six hours before transferring 20-30 worms to wells of a 96-well plate. Test agents were added and incubated with worms for 18 hours. Worms were sacrificed and the number of viable colony-forming units of MRSA USA300 in infected worms was determined for each treatment regimen. The figure presents the average percent reduction of MRSA USA300 for each treatment condition. Data shown in the graph were obtained from two independent experiments.

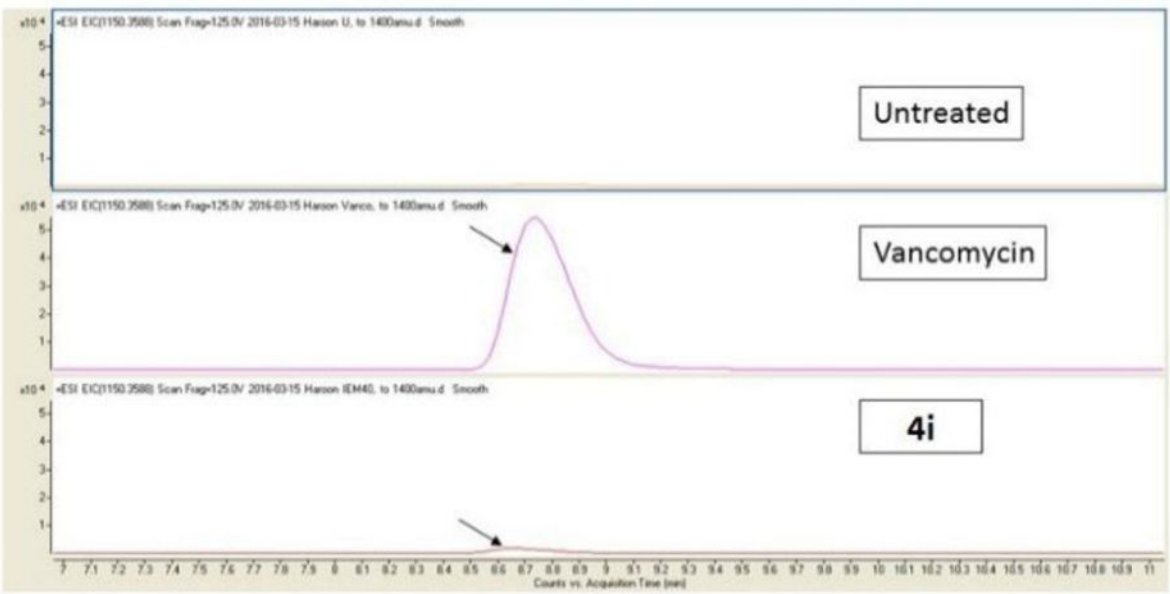

Figure 6. Detection of the final soluble cell wall precursor (UDP-*N*-acetylmuramyl pentapeptide) inside the cytoplasm of *S. aureus*

HPLC/MS chromatogram of *S. aureus* NRS107 (RN4220) treated with 10 × MIC of compound **4i** or vancomycin for 30 minutes. After centrifugation, the bacterial pellet was boiled for 30 minutes to release contents present in the bacterial cytoplasm. The lysate was analyzed using HPLC/MS, using a phenyl column, to determine the accumulation of the final soluble precursor in cell wall synthesis, UDP-*N*-acetylmuramyl pentapeptide (designated by the black arrows).

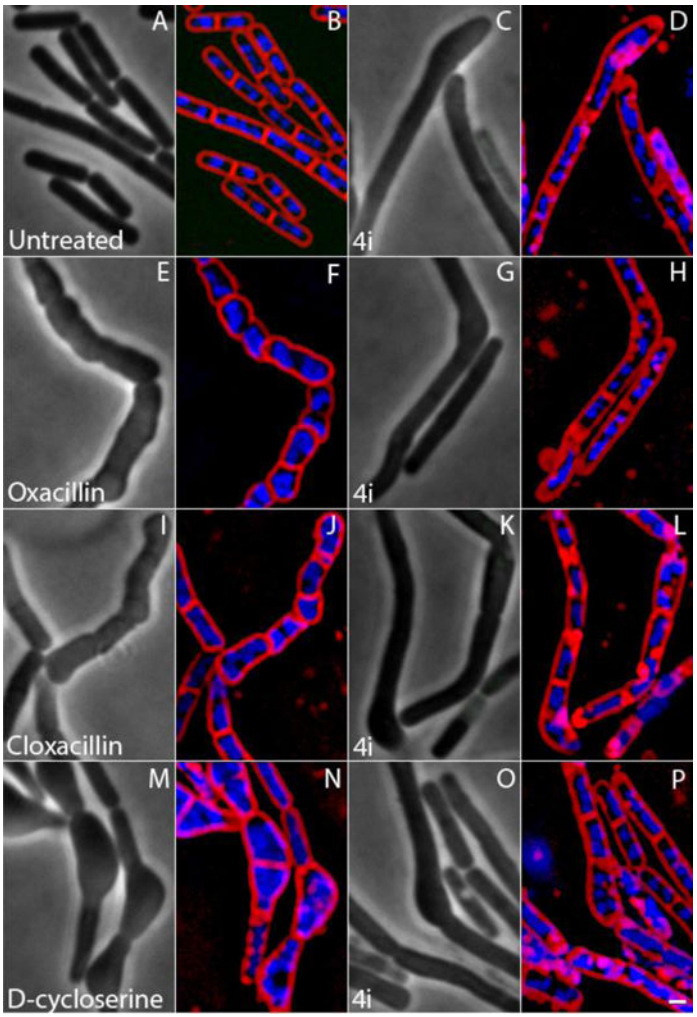

Figure 7. Compound 4i inhibits cell wall biosynthesis in *Bacillus subtilis*

All cells are grown at 37°C in LB-MSM and are shown at two hours. (A, B) Untreated cells. (E, F) Cells treated with oxacillin at 5×MIC (1.875 μg/mL). (I, J) Cells treated with cloxacillin at 1×MIC (0.47 μg/mL). (M, N) Cells treated with D-cycloserine at 1×MIC (37.5 μg/mL). (C, D, G, H, K, L, O, P,) Cells treated with **4i** at 4×MIC (3.5 μg/mL). Treatment with **4i** resulted in subtle cell shape defects and bulges consistent with cell wall inhibition. Cells were stained with FM 4−64 (red, to visualize cell membranes), DAPI (blue, to visualize DNA), and SYTOX Green (green, to confirm if the cell membrane had been lysed). Scale bar is 1 μm.

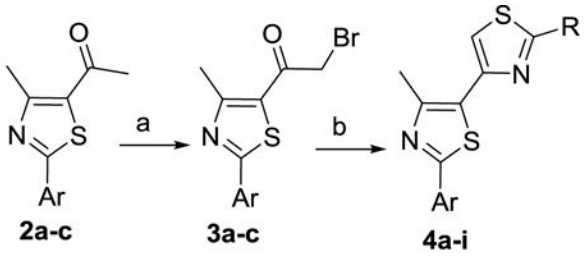

2a, 3a, Ar= *n*-butylphenyl
2b, 3b, Ar= biphenyl
2c, 3c, Ar= naphthyl
4a, Ar= *n*-butylphenyl, R = NH_2
4b, Ar= biphenyl, R = NH_2
4c, Ar= 2-naphthyl, R = NH_2
4d, Ar= *n*-butylphenyl, R = $NHNH_2$
4e, Ar= biphenyl, R = $NHNH_2$
4f, Ar= 2-naphthyl, R = $NHNH_2$
4g, Ar= *n*-butylphenyl, R = 
4h, Ar= biphenyl, R = 
4i, Ar= 2-naphthyl, R = 

Reagents and conditions: (a) AcOH, Br_2, 65-75 °C, 0.15 - 1 h; (b) appropriate thioamide, Absolute EtOH, K_2CO_3, heat at reflux, 4 - 8 h.

Scheme 1.

Table 1

The minimum inhibitory concentration (MIC in μg/mL) and the minimum bactericidal concentration (MBC μg/mL) of tested compounds screened against drug-resistant *S. aureus* clinical isolates.

	***S. aureus* NRS107 (RN4220)**		**MRSA NRS123 (USA400)**		**MRSA NRS382 (USA100)**		**MRSA NRS383 (USA200)**		**MRSA NRS384 (USA300)**		**VRSA4**		**VRSA10**	
Compound	**MIC**	**MBC**	**MIC**	**MBC**	**MIC**	**MBC**	**MIC**	**MBC**	**MIC**	**MBC**	**MIC**	**MBC**	**MIC**	**MBC**
4a	-	-	>64	>64	-	-	-	-	>64	>64	-	-	>64	>64
4b	-	-	>64	>64	-	-	-	-	>64	>64	-	-	>64	>64
4c	-	-	>64	>64	-	-	-	-	>64	>64	-	-	>64	>64
4d	16	32	16	16	-	-	-	-	16	16	-	-	>64	>64
4e	-	-	16	>64	8	>64	8	>64	16	64	-	-	16	16
4f	-	-	16	>64	8	>64	8	>64	16	64	-	-	16	16
4g	16	32	16	16	-	-	-	-	16	16	8	8	8	8
4h	16	32	16	16	-	-	-	-	8	16	8	8	8	8
4i	2	4	2	4	1	2	2	2	4	4	4	4	4	4
Linezolid	2	32	2	32	2	16	2	32	2	16	2	8	2	16
Vancomycin	1	1	1	1	<1	<1	1	1	1	1	>512	>512	>512	>512

Table 2

Metabolic stability analysis of compounds **1a** and **4i** in human liver microsomes

Tested compound	NADPH-Dependent CL_{int} (μL/min-mg)	NADPH-Dependent $T_{1/2}$ (min)	NADPH-Free CL_{int} (μL/min-mg)	NADPH-Free $T_{1/2}$ (min)
Lead compound (1a)	80.3	28.8	< 9.6	>240
4i	17.3	134	< 9.6	> 240